



HAL
open science

Triple-lobe wavelength fiber laser with a composite-state soliton regime

M. Kemel, A. Nady, G. Semaan, M. Salhi, F. Sanchez

► To cite this version:

M. Kemel, A. Nady, G. Semaan, M. Salhi, F. Sanchez. Triple-lobe wavelength fiber laser with a composite-state soliton regime. *Optics and Laser Technology*, 2021, 133, pp.106519 -. 10.1016/j.optlastec.2020.106519 . hal-03491537

HAL Id: hal-03491537

<https://hal.science/hal-03491537>

Submitted on 22 Aug 2022

HAL is a multi-disciplinary open access archive for the deposit and dissemination of scientific research documents, whether they are published or not. The documents may come from teaching and research institutions in France or abroad, or from public or private research centers.

L'archive ouverte pluridisciplinaire **HAL**, est destinée au dépôt et à la diffusion de documents scientifiques de niveau recherche, publiés ou non, émanant des établissements d'enseignement et de recherche français ou étrangers, des laboratoires publics ou privés.



Distributed under a Creative Commons Attribution - NonCommercial 4.0 International License

Triple-lobe wavelength fiber laser with a composite-state soliton regime

M. Kemel^a, A. Nady^{a,b,*}, G. Semaan^a, M. Salhi^{a,*} and F. Sanchez^a

^aUniversité d'Angers, Laboratoire de Photonique d'Angers, E. A. 4464, 2 Boulevard Lavoisier, 49045 Angers, France.

^bDepartment of Physics, Faculty of Science, Beni-Suef University, 62511 Beni-Suef, Egypt.

*Corresponding author: mohamed.salhi@univ-angers.fr & ahmed.nadi93@yahoo.com

It is a shared correspondence between M. Salhi and A. Nady.

Abstract

We report the experimental study of triple-lobe wavelength double-clad co-doped Er:Yb fiber laser operating with a composite-state soliton regime. The passively mode-locked emission is achieved through nonlinear polarization rotation (NPR) technique. The three-lobe wavelengths oscillation, centred at 1567 nm, 1585 nm, and 1616 nm, is attributed to two phenomena; the nonlinear filtering based on intensity-dependent polarization rotation and the linear loss of the cavity impacting the population inversion (gain). Moreover, by fine adjustment of the polarization controllers, this complex regime still can be switched into harmonic states. This work shows a novel operation regime, which could help understanding the composite soliton dynamics in fiber lasers and could be useful for different applications in wavelength division multiplexed transmission systems and optical signal processing.

Keywords: Mode-locked fiber laser; Multi-wavelength lasers; Composite-state soliton

1. Introduction

Due to its compactness, low-cost configuration, power efficiency, and excellent beam quality, mode-locked fiber laser as a complex nonlinear system provides an ideal platform for investigating the enormous variety of soliton dynamics [1]. It enables the generation of well-shaped pulses organized in harmonic solitons [2, 3], soliton rains [4, 5], soliton molecules [6, 7], and soliton crystals [8, 9]. It is also possible to obtain a coexistence of different soliton states by manipulating the laser cavity parameters. For instance, the coexistence of chaotic and regular soliton structure in fiber lasers has been theoretically predicted [10]. Tang et al. investigated experimentally the coexistence of two types of soliton shape based on dispersion management in near zero dispersion regime [11]. Then, Wang reported on the coexistence of bright pulses and dark solitons in Er-doped fiber laser (EDFL) with strong normal cavity dispersion [12]. Moreover, different soliton patterns inside the same signal can simultaneously coexist. In Ref [13], the coexistence of alternate crystal and liquid soliton phases was experimentally observed.

1 Meanwhile, in an ultra-large net anomalous dispersion EDFL, the demonstration of the
2 coexistence of strong and weak pulses has been reported [14]. In addition, the simultaneous
3 generation of harmonic soliton molecules with rectangular noise-like pulses and the coexistence
4 of high repetition rate harmonic mode-locking with noise-like pulse have been demonstrated [15,
5 16]. In 2018, the coexistence of dissipative soliton and stretched pulse was also observed in a
6 dual-wavelength Tm-doped fiber laser [17]. Very recently, the emission of multi-state solitons
7 (soliton singlets and molecules) in a dual-wavelength EDFL laser has been reported by Liu et al.
8 [18]. All these works were carried out in lasers operating with single or dual-lobe wavelength.

9 Multi-lobe wavelength fiber lasers can provide an excellent platform for the generation of
10 composite soliton regime with several stable coexisting patterns. Apart from the composite soliton
11 regime, the multi-wavelength fiber lasers and multi-wavelength comb lasers are of a great interest
12 for their potential in various applications and were respectively studied in the framework of either
13 a continuous regime emission or a modulated single-lobe wavelength [19-21]. Basically, from a
14 C-band fiber amplifier, the laser operates in single-lobe spectrum in the wavelength ranging from
15 1525 nm to 1565 nm. However, manipulating the nonlinear filtering effect based on intensity-
16 dependent polarization rotation enables the generation of double-lobe wavelength oscillation [18,
17 22]. Furthermore, by controlling the linear intracavity loss, a wide tunable EDFL (covering
18 (C+L)-band) based on a C-band amplifier has been demonstrated [23]. So, we can conclude that
19 the laser performance in terms of the number of operating wavelengths can be controlled by the
20 adjustment of both the nonlinear filtering and linear loss of the cavity.

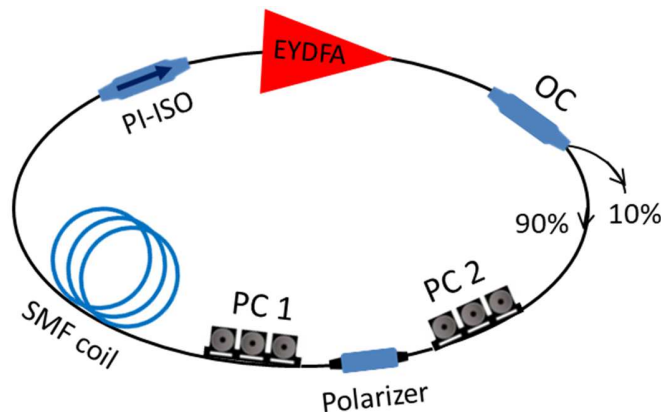
21 In this paper, we demonstrate the generation of composite soliton distribution with a triple-lobe
22 wavelength spectrum in mode-locked EDFL based on both nonlinear filtering and linear loss
23 management of the cavity. The obtained results show the generation of wavelength-dependent
24 domains with well-separated three distinct wavelength-lobe and composite soliton operation. This
25 research brings new study to the composite-state soliton regime formed from three-lobe
26 wavelength.

27 **2. Experimental setup**

28 The experimental setup of the proposed regime is schematically illustrated in Fig. 1. It is a
29 unidirectional ring (UR) laser cavity enabling the generation of triple-lobe wavelength mode-
30 locked laser using nonlinear polarization rotation (NPR) mechanism configured by a set of
31 polarizer and two polarization controllers (PC1 and PC2). The cavity includes a C-band double-
32
33

1 clad co-doped Er:Yb 30 dBm fiber amplifier (EYDFA) built by Lumibird company (KPS-BT2-C-
2 30-BO-FA). The total cavity length is around 304 m (corresponding to a round-trip time of 1.52
3 μ s) consisting of a double clad fiber of 5 m with -0.021 ps²/m second-order dispersion and 285 m
4 single mode fiber (SMF28) coil with second-order dispersion of -0.022 ps²/m. The net cavity
5 dispersion is about -6.683 ps². A polarization insensitive isolator (PI-ISO) was used to ensure the
6 unidirectional propagation of the light.

7 The laser output characteristics are simultaneously monitored by an optical spectrum analyzer
8 (Anritsu MS9740A, 0.6 μ m-1.7 μ m), a 13-GHz oscilloscope (Agilent infinium DSO8130B)
9 combined with two 12-GHz photo-detectors (TTI, Model TIA61200 O/E Converter), a high
10 power integrating sphere (Thorlabs S146C), and an electronic spectrum analyzer (Rohde &
11 Schwarz FSP Spectrum Analyzer 9 kHz to 13.6 GHz). A manually optical tunable filter (OTF)
12 with filter bandwidth of 0.5 nm and tuning range from 1500 to 1630 nm (SANTEC OTF 320) is
13 inserted at the output of the cavity for wavelength-resolved measurements.



14 Fig. 1. Experimental setup of the unidirectional ring laser cavity.

15 3. Results and discussion

16 The experiment was conducted thoughtfully in such a way to obtain multi-wavelength operation.
17 This is achieved by using a long cavity (304 m) to support narrow artificial filtering that facilitates
18 the multi-wavelength operation. In addition, the cavity loss was controlled to enhance the gain in
19 L-band since the gain coefficient of EDF in L-band is much lower than that in C-band [22, 24-26].
20 To have enough gain in both C- and L-bands, a 10 % output coupler (OC) was used.

21 In the beginning, self-started mode-locking was obtained at pump power of 0.27 W. By
22 appropriate adjustment of the PCs with further increasing the pump power from 0.27 W to 0.8 W,
23
24
25
26

1 the spectrum has grown into triple-lobe wavelength regime as depicted in Fig. 2(a). Initially, at
2 pump power of 0.27 W, the optical spectrum shows two peaks located at 1567 nm and 1585 nm.
3 These peaks are associated respectively to a continuous wave and a soliton clusters with narrow
4 square shape as seen in the corresponding temporal trace (black trace in Fig. 2(b)). When the
5 pump power reached 0.37 W, the triple-lobe wavelength regime starts to build up where three
6 distinct spectral lobes appear at ~1567 nm, ~1585 nm, and ~1616 nm (1567 nm is a characteristic
7 of a soliton regime with Kelly sidebands while 1585 nm and 1616 nm are smooth). At the pump
8 power of 0.8 W, the triple-lobe wavelength regime was completely formed, and different
9 coexisting soliton patterns were observed on the oscilloscope.

10 The physical process behind such spectrum dynamics is mainly attributed to the significant
11 birefringence in the cavity which exhibits artificial spectral filtering, and to the intracavity linear
12 loss that shifts the lasing at longer wavelength (1616 nm). In fact, the oscillation threshold of
13 about 0.27 W is reached first for wavelength-lobes at ~1567 nm and ~1585 nm due to
14 compensation of the loss by the gain. The threshold level of about 0.37 W at ~1616 nm is reached
15 later because the gain in this spectral region is not enough at 0.27 W pump power.

16 To study the effect of intracavity linear loss and how it affects the regime, an optical attenuator
17 was inserted in the cavity to introduce additional loss, Γ . This is a way to control the number of
18 wavelength lobes as shown in Fig. 3. For example, at $\Gamma= 0.3$ dB, the spectrum exhibits three
19 wavelength lobes and by increasing loss in the cavity we can suppress one of these wavelengths as
20 shown in the red trace (at $\Gamma= 0.5$ dB) and blue trace (at $\Gamma= 0.4$ dB). This shows different
21 contribution of each wavelength in the triple-wavelength spectrum as seen in the temporal trace of
22 Fig. 3(b).

23

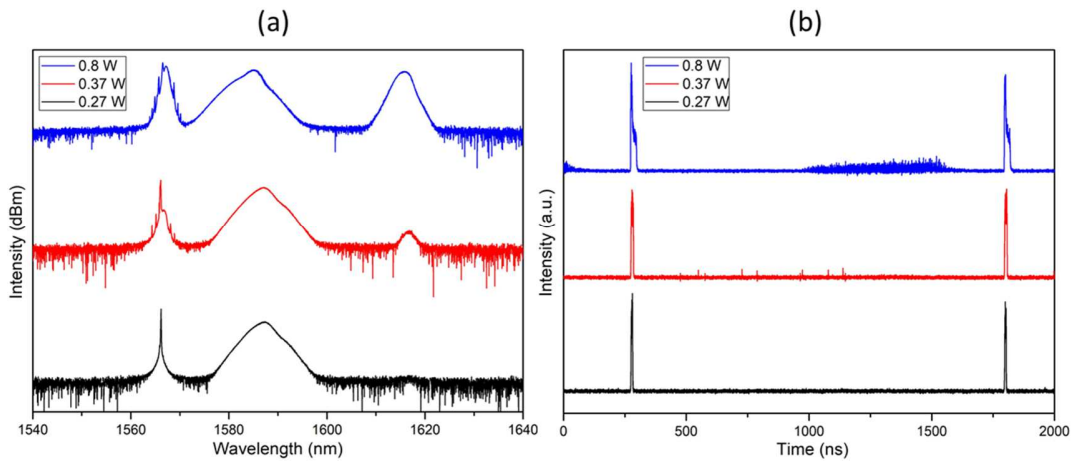


Fig. 2. Evolution of spectrum (a) and the corresponding oscilloscope trace (b) at different values of pump power.

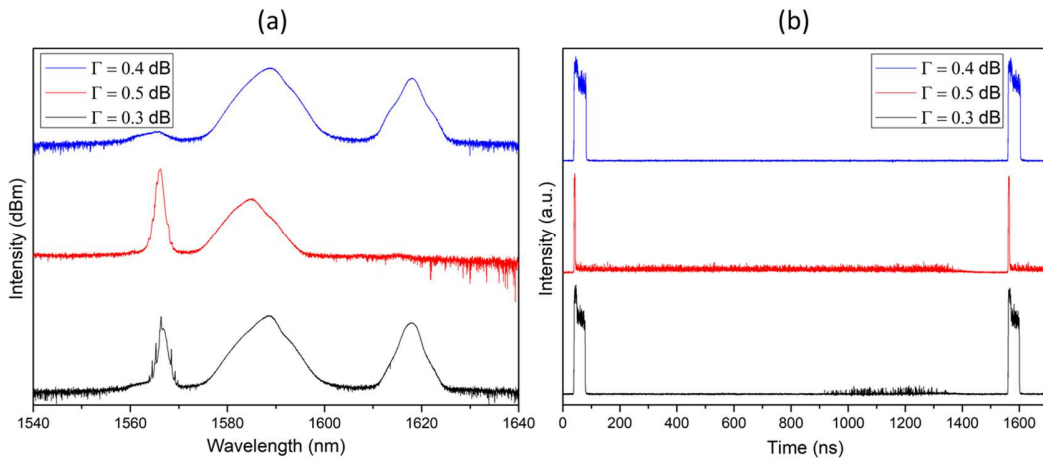
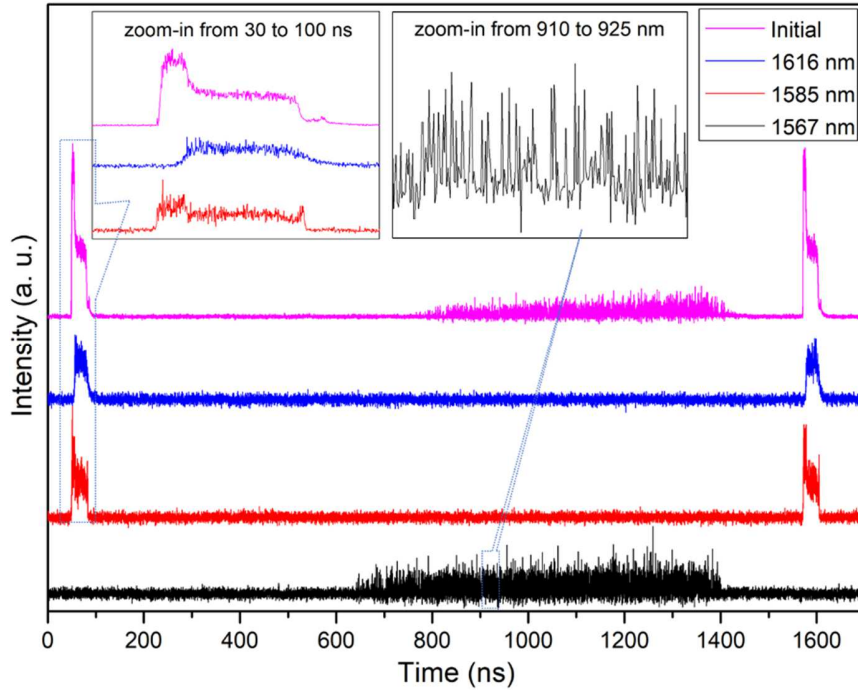


Fig. 3. Optical spectra (a) and the corresponding temporal traces (b) at fixed pump power but for different intracavity loss.

In order to further investigate the contribution of each wavelength in the spectrum, OTF was used to conduct wavelength-resolved measurements. Figure 4 shows the temporal trace of the filtered signals at 0.8 W. Unresolved bunch of solitons represented by the black-curve trace are obtained at 1567 nm. This appears more clearly in the zoom-in of the black trace. The temporal traces at 1585 nm and 1616 nm are represented by the red and blue-curves, and respectively show a square condensed phase soliton with the same group velocity, which can be separated using an optical filter. In general, pulse trains corresponding to different wavelengths should have different group velocities owing to the group velocity dispersion of the cavity, which results in different fundamental repetition frequencies on the RF spectrum [27]. However, our results demonstrate

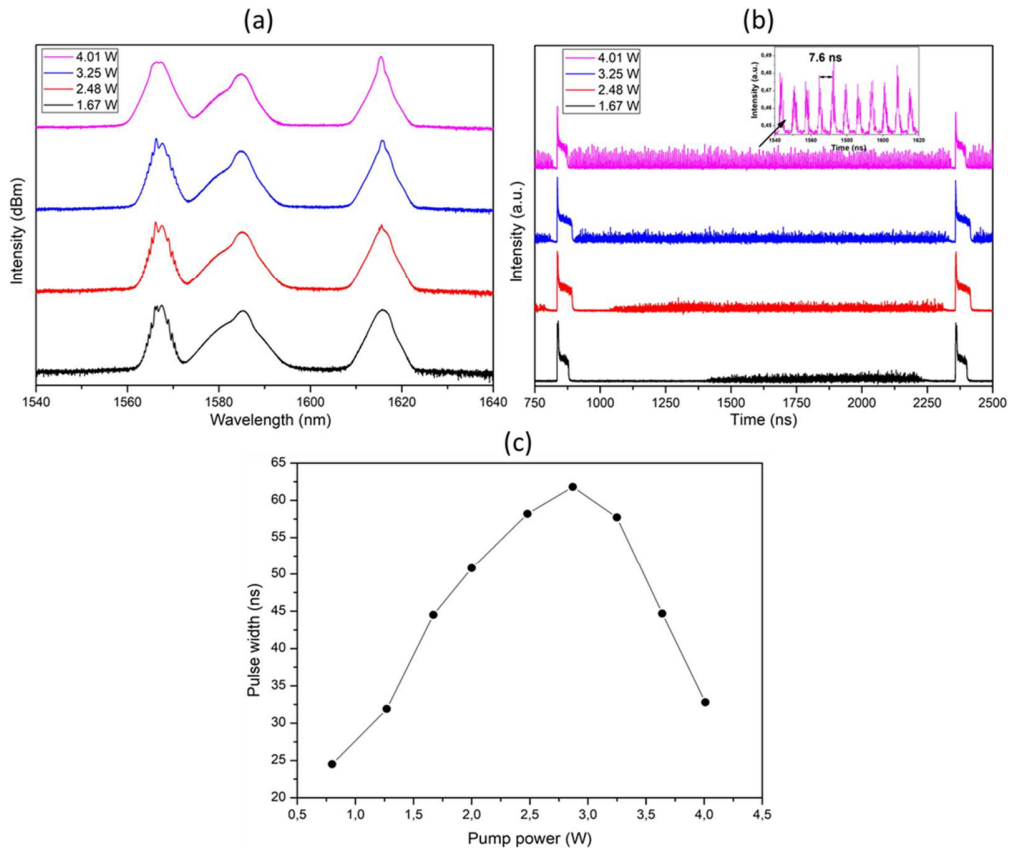
1 that, the pulse ensembles are trapped together and coexist in the cavity; they co-propagate as a
2 non-dispersive unit although they have different central wavelengths. This indicates that the pulse
3 ensembles are group velocity locked.



4
5
6
7
8

Fig. 4. Temporal trace of the initial and filtered signal.

9 We have also investigated the effect of the pump power on the characteristics of the presented
10 laser regime. Figure 5 illustrates the evolution of spectrum and the corresponding oscilloscope
11 trace versus the pump power. When the pump power was increased from 0.8 W to 3.2 W, the
12 spectrum presented in Fig. 5(a) reveals the same dynamics as mentioned before, whereas the
13 square pulse width increases, and the soliton bunch spreads over almost the whole cavity as
14 shown in Fig. 5(b). At pump power higher than 3.2 W, the spectrum located at 1567 nm becomes
15 smooth with no sideband and the square pulse width reduces to 32.8 ns at 4 W pump power. The
16 variation of the square pulse width is clearly identified in Fig. 5(c), where pulse width is tuned
17 from 24.5 ns to 61.8 ns before 3.2 W, and then decreases to 32.8 ns at 4 W. The boost in energy
18 reduces the square pulse duration and increases the number of pulses in the soliton bunch forming
19 high repetition rate harmonic of fine soliton bunches with a period of ~ 7.6 ns as shown in the inset
20 of Fig. 5(b).



1
 2 Fig. 5. Evolution of the spectrum (a), the corresponding oscilloscope trace (b), and square pulse
 3 width (c) at different values of pump power.

4
 5 Figure 6 depicts the RF spectrum at the pump power of ~ 4 W, in which the repetition frequency is
 6 ~ 656.4 kHz corresponding to the fundamental repetition rate of the cavity with a signal to noise
 7 ratio (SNR) of ~ 62 dB, which manifests the good stability of the coexistence patterns. The inset of
 8 Fig. 6 illustrates the signal envelope with 250 MHz span. It shows another frequency peak at
 9 ~ 139.5 MHz, which corresponds to the repetition frequency of the high repetition rate harmonic
 10 pulses of the soliton centered at 1567 nm.

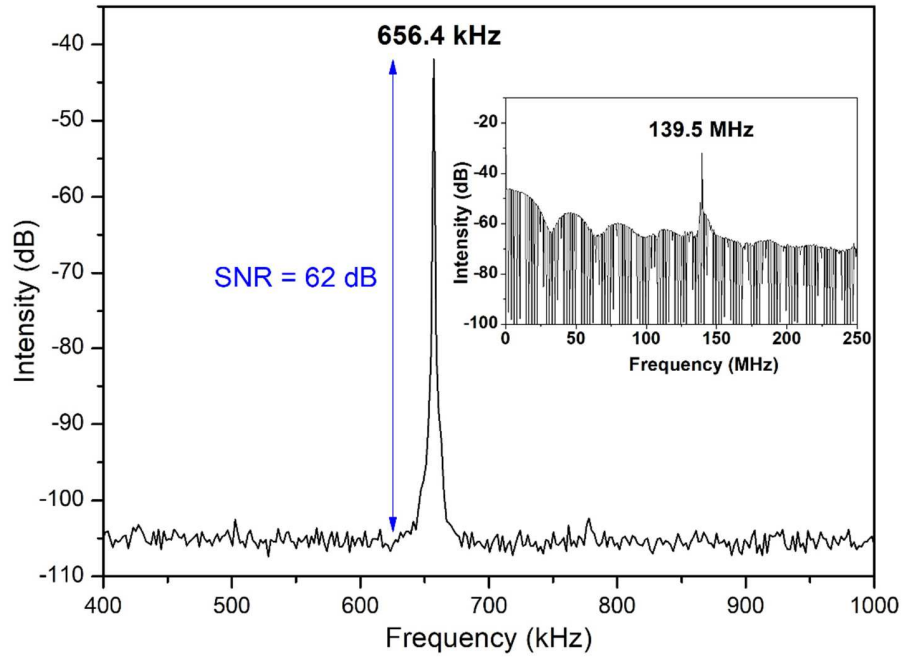


Fig. 6. RF spectrum at the pump power of 4 W. Inset: RF spectrum over a 250 MHz span.

Further investigation of this regime reveals that only by fine adjustment of the PCs, harmonic states of the presented regime can be generated. Figure 7 shows the optical spectra and the corresponding temporal traces of different harmonic orders at pump power of 3.2 W. Their periods are ~ 770 ns, ~ 378 ns, and ~ 189 ns, which represent the 2nd harmonic, 4th harmonic, and 8th harmonic, respectively observed on the oscilloscope (Fig. 7(b)). The switch from one harmonic to other can be performed by fine adjustment of PCs. This adjustment causes very small shift towards shorter wavelengths as shown in Fig. 7(a), since it modifies the characteristics of the nonlinear transmission curve of the artificial filtering.

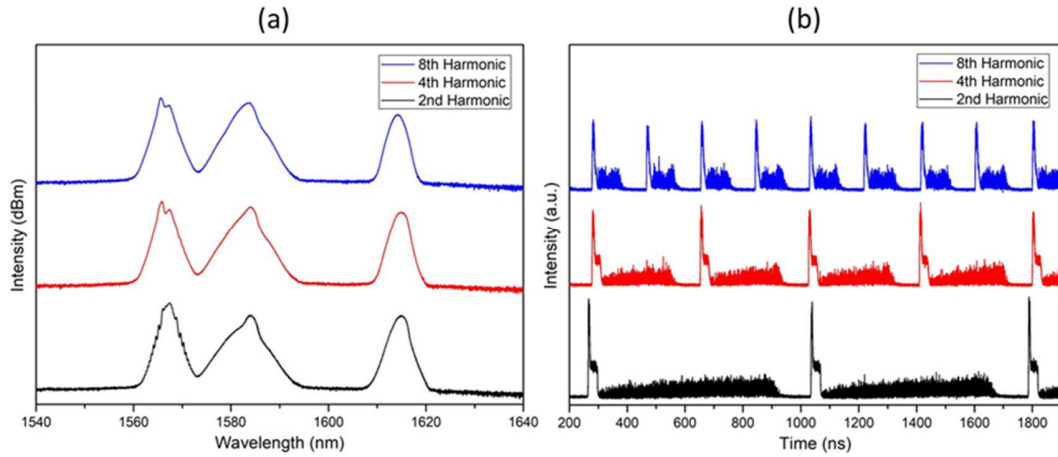


Fig. 7. Optical Spectra (a) and temporal traces (b) of harmonic states at the pump power of 3.2 W.

4. Conclusions

We experimentally demonstrated the coexistence of different soliton states in a triple-wavelength mode-locked EDFL based on NPR technique. The spectrum exhibits three distinct well-separated spectral peaks centered at 1567 nm, 1585 nm, and 1616 nm. By means of an optical tunable filter, we confirmed that each soliton pattern corresponds to a specific spectral lobe. The introduced regime is operated at fundamental repetition rate of 656.4 kHz. Besides, by carefully adjusting the PCs, it can evolve into different harmonic states. This work shows a novel operation regime, which could enrich understanding the composite state soliton dynamics and could be useful for various applications in wavelength division multiplexed transmission systems and optical signal processing.

Declaration of Competing Interests

The authors declare that they have no known competing financial interests or personal relationships that could have appeared to influence the work reported in this paper.

Acknowledgments

The authors acknowledge Université Bretagne Loire and Université d'Angers for co-funding the post-doctoral fellowship of Dr. Ahmed Nady.

References

1. Grelu, P. and N. Akhmediev, *Dissipative solitons for mode-locked lasers*. Nature photonics, 2012. **6**(2): p. 84.
2. Lecaplain, C. and P. Grelu, *Multi-gigahertz repetition-rate-selectable passive harmonic mode locking of a fiber laser*. Optics express, 2013. **21**(9): p. 10897-10902.
3. Wang, X., et al., *Experimental study on buildup dynamics of a harmonic mode-locking soliton fiber laser*. Optics express, 2019. **27**(20): p. 28808-28815.
4. Chouli, S. and P. Grelu, *Rains of solitons in a fiber laser*. Optics express, 2009. **17**(14): p. 11776-11781.
5. Niang, A., et al., *Rains of solitons in a figure-of-eight passively mode-locked fiber laser*. Applied Physics B, 2014. **116**(3): p. 771-775.
6. Zavyalov, A., et al., *Dissipative soliton molecules with independently evolving or flipping phases in mode-locked fiber lasers*. Physical Review A, 2009. **80**(4): p. 043829.
7. Stratmann, M., T. Pagel, and F. Mitschke, *Experimental observation of temporal soliton molecules*. Physical review letters, 2005. **95**(14): p. 143902.
8. Amrani, F., et al., *Dissipative solitons compounds in a fiber laser. Analogy with the states of the matter*. Applied Physics B, 2010. **99**(1-2): p. 107-114.
9. Amrani, F., et al., *Passive harmonic mode locking of soliton crystals*. Optics letters, 2011. **36**(21): p. 4239-4241.
10. Akhmediev, N., J.M. Soto-Crespo, and G. Town, *Pulsating solitons, chaotic solitons, period doubling, and pulse coexistence in mode-locked lasers: Complex Ginzburg-Landau equation approach*. Physical Review E, 2001. **63**(5): p. 056602.
11. Tang, D., et al., *Coexistence and competition between different soliton-shaping mechanisms in a laser*. Physical Review A, 2007. **75**(6): p. 063810.
12. Wang, L., *Coexistence and evolution of bright pulses and dark solitons in a fiber laser*. Optics Communications, 2013. **297**: p. 129-132.
13. Amrani, F., et al., *Intricate solitons state in passively mode-locked fiber lasers*. Optics express, 2011. **19**(14): p. 13134-13139.
14. Liu, X., *Coexistence of strong and weak pulses in a fiber laser with largely anomalous dispersion*. Optics express, 2011. **19**(7): p. 5874-5887.
15. Huang, Y.-Q., et al., *Coexistence of harmonic soliton molecules and rectangular noise-like pulses in a figure-eight fiber laser*. Optics letters, 2016. **41**(17): p. 4056-4059.
16. Wang, Y., et al., *Coexistence of noise-like pulse and high repetition rate harmonic mode-locking in a dual-wavelength mode-locked Tm-doped fiber laser*. Optics express, 2017. **25**(15): p. 17192-17200.
17. Wang, Y., et al., *Coexistence of dissipative soliton and stretched pulse in dual-wavelength mode-locked Tm-doped fiber laser with strong third-order dispersion*. Optics express, 2018. **26**(14): p. 18190-18201.
18. Liu, B., et al., *Coexistence of soliton singlets and molecules in a dual-wavelength mode-locked fiber laser*. Optics Communications, 2020. **457**: p. 124700.
19. Zhou, K., et al., *Room-temperature multiwavelength erbium-doped fiber ring laser employing sinusoidal phase-modulation feedback*. Optics letters, 2003. **28**(11): p. 893-895.
20. Zhang, Z., L. Zhan, and Y. Xia, *Multiwavelength comb generation in self-starting passively mode-locked fiber laser*. Microwave and Optical Technology Letters, 2006. **48**(7): p. 1356-1358.
21. Feng, X., et al., *Mechanism for stable, ultra-flat multiwavelength operation in erbium-doped fiber lasers employing intensity-dependent loss*. Optics & Laser Technology, 2012. **44**(1): p. 74-77.

- 1 22. Horowitz, M. and Y. Silberberg, *Nonlinear filtering by use of intensity-dependent polarization*
2 *rotation in birefringent fibers*. Optics letters, 1997. **22**(23): p. 1760-1762.
- 3 23. Meng, Y., et al., *Mode-locked Er: Yb-doped double-clad fiber laser with 75-nm tuning range*.
4 Optics letters, 2015. **40**(7): p. 1153-1156.
- 5 24. Dong, X., et al., *Output power characteristics of tunable erbium-doped fiber ring lasers*. Journal of
6 lightwave technology, 2005. **23**(3): p. 1334.
- 7 25. Guesmi, K., et al., *1.6 μm emission based on linear loss control in a Er: Yb doped double-clad fiber*
8 *laser*. Optics letters, 2014. **39**(22): p. 6383-6386.
- 9 26. Meng, Y., et al., *Color domains in fiber lasers*. Optics letters, 2018. **43**(20): p. 5054-5057.
- 10 27. Wang, Y., et al., *Tunable and switchable dual-wavelength mode-locked Tm 3+-doped fiber laser*
11 *based on a fiber taper*. Optics express, 2016. **24**(14): p. 15299-15306.
12